Available online at www.sciencedirect.com
SCIENCE DIRECT®
Catalysis Today 85 (2003) 207–218
CATALYSIS TODAY
www.elsevier.com/locate/cattod

Co^0 from partial reduction of $La(Co,Fe)O_3$ perovskites for Fischer–Tropsch synthesis

L. Bedel [a], A.C. Roger [a,*], C. Estournes [b], A. Kiennemann [a]

[a] *LMSPC ECPM, Laboratoire des Matériaux, Surfaces et Procédés pour la Catalyse, UMR 7515, 25, rue Becquerel, 67087 Strasbourg Cedex 2, France*

[b] *GMI IPCMS, Groupe des Matériaux Inorganiques, Institut de Physique et Chimie des Matériaux de Strasbourg, UMR 7504, 23 rue du Loess 67037 Strasbourg Cedex, France*

Received 7 February 2003; received in revised form 14 March 2003; accepted 14 March 2003

Abstract

Small Co clusters ($d < 10$ nm) supported over mixed La–Co–Fe perovskites were successfully synthesized. These catalysts were active for Fischer–Tropsch (FT). Depending on the Co to Fe ratios the mixed perovskite exhibited two different forms: the rhombohedral phase of $LaCoO_3$ is maintained for the mixed perovskite when $x > 0.5$, the orthorhombic phase of $LaFeO_3$ is found for $x < 0.5$. Interestingly only one of these structures is active for the FT reaction: the orthorhombic structure. This is most likely due to the capacity of this material to maintain its structure even with a high number of cation vacancies. These cations (mostly Co) were on purpose extracted and reduced. Magnetic measurements clearly showed their metallic nature. Rhombohedral Co–Fe mixed perovskites ($x \geq 0.5$) cannot be used as precursors for Fischer–Tropsch catalysts: their partial reduction only consists in a complete reduction of Co^{3+} into Co^{2+}.

The partial reduction of orthorhombic perovskites ($x < 0.5$) leads to active Fischer–Tropsch (FT) catalysts by formation of a metal phase well dispersed on a cation-deficient perovskite. The FT activity is related to the stability of the precursor perovskite. When initially calcined at 600 °C, a maximum of 8.6 wt.% of Co^0 can be extracted from $LaCo_{0.40}Fe_{0.60}O_3$ (compared to only 2 wt.% after calcination at 750 °C). The catalyst is then composed of Co^0 particles of 10 nm on a stable deficient perovskite $LaCo_{0.05}{}^{3+}Fe_{0.60}{}^{3+}O_{2.40}$. Catalytic tests showed that up to 70% in the molar selectivity for hydrocarbons was obtained at 250 °C, 40% of which was composed of the C_2–C_4 fraction.

Keywords: Fischer–Tropsch synthesis; Perovskites; Partial reduction

1. Introduction

Perovskites are well known catalysts for numerous oxidation reactions. These include total and partial oxidation of methane and carbon monoxide oxidation [1–8]. They are also used for alkene hydrogenation [9] and alkane hydrogenolysis [10] reactions. In the present work mixed perovskite oxides are found as active Fischer–Tropsch catalysts. Cobalt and iron, the two most used metals for Fischer–Tropsch synthesis, under the form of trivalent cations have ionic radii which allow their crystallization in a perovskite ABO_3 structure when combined with lanthanum in the A-sites [11,12] (see Scheme 1). The perovskite structure is very versatile and can stand many crystalline defects. More specially, this structure allows cationic vacancies [13–16]. This ability has motivated the

* Corresponding author. Fax: +33-3-90-24-27-69.
E-mail address: rogerac@ecpm.u-strasbg.fr (A.C. Roger).

0920-5861/$ – see front matter © 2003 Elsevier B.V. All rights reserved.
doi:10.1016/S0920-5861(03)00388-2

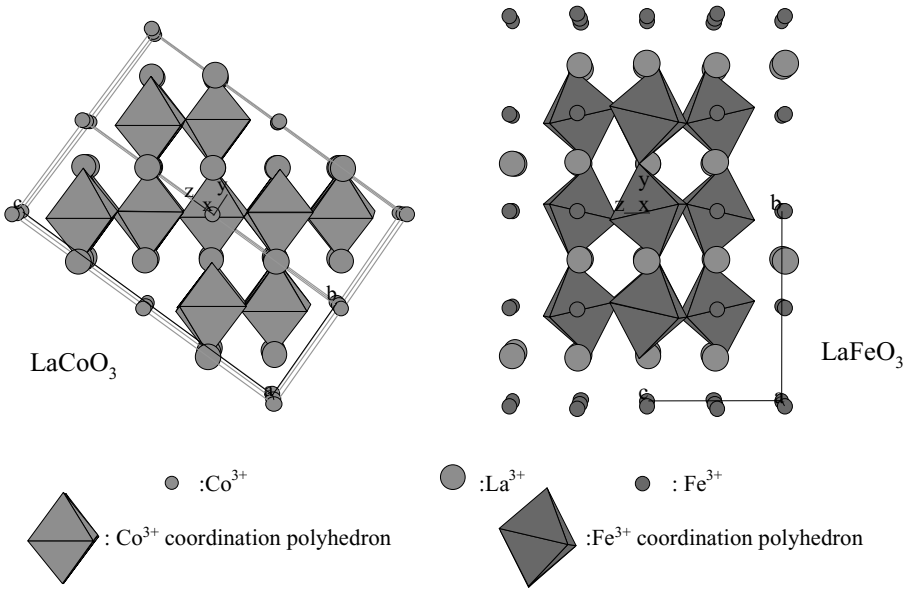

Scheme 1. Perovskite lattice of $LaCoO_3$ and $LaFeO_3$.

present investigation, despite a cation extraction by reduction of cobalt or iron cations from the "precursor" perovskite material to generate a nanometallic phase was made possible. In this work, mixed $La(Co_xFe_{1-x})O_3$ perovskites are synthesized by a sol–gel like method to ensure a good homogeneity of the mixed oxides. The reducibility of these precursor perovskites is studied by TPR and magnetic measurements. The Fischer–Tropsch activity of such partially reduced perovskites is then presented for the more active systems in addition to CO dissociation studies.

2. Experimental

2.1. Catalyst preparation

The perovskites $LaCo_xFe_{(1-x)}O_3$ were prepared by thermal decomposition of mixed La, Co and Fe propionates. This preparation method is derived from the sol–gel method and based on the oligomerization of propionate precursors in propionic acid [17]. The starting materials for La, Co and Fe were La^{III} acetate, Co^{II} acetate and Fe^0 powder, which all led to propionate precursors in propionic acid [18]. The three boiling solutions were mixed and propionic acid was evaporated until a resin was obtained. The resin was calcined ($2\,^{\circ}C\,min^{-1}$) under air at 600, 750 or 1100 °C for 6 h.

The amount of cobalt versus iron cations in the B sites of the perovskite was varied between $x = 0$ ($LaFeO_3$) and $x = 1$ ($LaCoO_3$) (see Table 1).

2.2. Catalyst characterization

2.2.1. Morphology (SEM)

The catalysts were studied by scanning electron microscopy (SEM) on a JEOL scanning electron microscope. The composition was determined by means of energy-dispersive X-ray spectroscopy (EDXS).

Table 1
Comparison of the theoretical and experimental (EDXS) perovskite compositions

	Theoretical composition	Real composition
$x = 0$	$LaFeO_3$	$LaFeO_3$
$x = 0.25$	$LaCo_{0.25}Fe_{0.75}O_3$	$LaCo_{0.24}Fe_{0.76}O_3$
$x = 0.4$	$LaCo_{0.40}Fe_{0.60}O_3$	$LaCo_{0.40}Fe_{0.60}O_3$
$x = 0.5$	$LaCo_{0.50}Fe_{0.50}O_3$	$LaCo_{0.49}Fe_{0.51}O_3$
$x = 0.6$	$LaCo_{0.60}Fe_{0.40}O_3$	$LaCo_{0.59}Fe_{0.41}O_3$
$x = 0.75$	$LaCo_{0.75}Fe_{0.25}O_3$	$LaCo_{0.74}Fe_{0.26}O_3$
$x = 1$	$LaCoO_3$	$LaCoO_3$

2.2.2. Specific surface area (BET)

Specific area measurements were carried out by using the BET method based on the N_2 physisorption capacity at 77 K on Coulter SA 3100 apparatus.

2.2.3. X-ray diffraction (XRD)

X-ray diffraction data were collected at room temperature on a Siemens D5000 diffractometer using the Cu Kα radiation.

2.3. Catalyst reducibility

2.3.1. Thermoprogrammed reduction

The thermoprogrammed reductions (TPR) were carried out on 50 mg of catalyst heated from 25 to 900 °C (15 °C min^{-1}) under 10%H_2/He (total gas flow: 50 ml min^{-1}).

2.3.2. Magnetic measurements

Magnetic measurements were performed between 25 and 950 °C (10 °C min^{-1}) under the same reducing flow as in TPR, under a magnetic field of 10 000 Oe.

Magnetization cycles were carried out at room temperature by varying the magnetic field from −10 000 to 10 000 Oe.

2.4. Catalytic test

2.4.1. CO disproportionation

CO disproportionation on partially reduced perovskites was carried out. The reducing pretreatment consisted on heating a 100 mg samples until 450 °C (2 °C min^{-1}) under 10% of H_2 (5 ml min^{-1}) in He (45 ml min^{-1}). When 450 °C were reached, the H_2 flow was stopped and the He flow was decreased down to 30 ml min^{-1}. The temperature was decreased at 350 °C. Successive CO pulses (0.5 ml) were then injected on the sample, the CO conversion and the CO_2 formation were determined by gas chromatography.

2.4.2. Fischer–Tropsch synthesis

Catalytic tests under CO/H_2 were performed in a fixed bed reactor at 1 MPa pressure. A 300 mg of catalyst was first heated up to 450 °C (2 °C min^{-1}) under a reducing flow (10% H_2/N_2 at total flow of 50 ml min^{-1}) at atmospheric pressure and maintained for 90 min. Hydrogen flow was then stopped and temperature was decreased down to 200 °C. At this temperature, the pressure was increased to 1 MPa. Then the N_2 was replaced by the CO/H_2 (1:1) mixture with a GHSV of 3000 h^{-1}. The catalytic tests were carried out between 250 and 340 °C, 60 h for each temperature at the steady state, after 60 h of stabilization. The reaction products were analyzed on line by TCD gas chromatography.

3. Results and discussion

3.1. Morphology and bulk composition (SEM)

Scanning electron microscopy observations of the perovskites after calcination at various temperatures show that particles are monodisperse and of spherical shape (see Fig. 1 for $LaFeO_3$ and $LaCoO_3$ (calcined at 750 °C)). The mean particle diameter linearly increases from 100 nm for $LaFeO_3$ ($x = 0$) to 200 nm for $LaCoO_3$ ($x = 1$) for the series of perovskites.

The composition of the oxides determined by EDXS analysis is given in Table 1. Due to the preparation method which does not include any separation step (crystallization, filtration, etc.), the compositions are consistent with the expected values.

3.2. Specific surface area (BET)

The specific surface area of the $LaCo_xFe_{(1-x)}O_3$ perovskites (calcination at 750 °C) (Fig. 2) is low, and ranges from 8.8 to 3.9 $m^2\,g^{-1}$ from $LaFeO_3$ ($x = 0$) to $LaCoO_3$ ($x = 1$). The specific surface areas correspond to the geometrical surfaces of the spherical particles, indicating that the grains are nonporous.

For the perovskite series heated at 600 °C, the specific surface areas also decrease with increasing cobalt content, and vary between 23 and 15 $m^2\,g^{-1}$ from $LaFeO_3$ to $LaCoO_3$.

3.3. X-ray diffraction (XRD)

$LaFeO_3$ and $LaCoO_3$ do not crystallize in the same space group. $LaFeO_3$ is orthorhombic [11], with a main diffraction peak at $d = 2.772$ Å ((1 2 1) plane). $LaCoO_3$ is rhombohedral [12], with

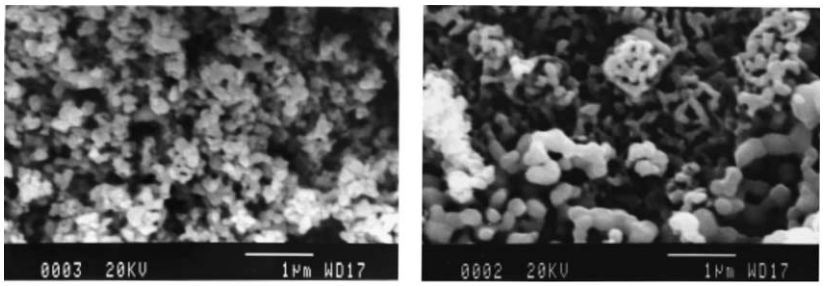

Fig. 1. SEM observation of (a) $LaFeO_3$ calcined at 750 °C, (b) $LaCoO_3$ calcined at 750 °C.

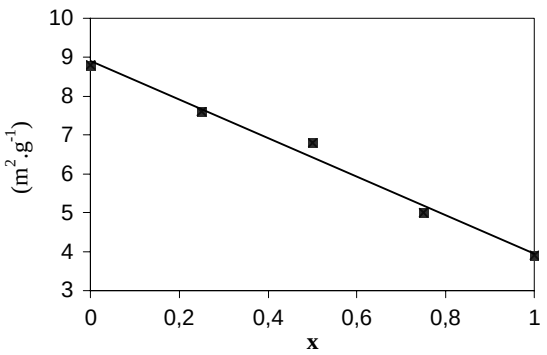

Fig. 2. Specific surface area of $LaCo_xFe_{(1-x)}O_3$ after calcination at 750 °C.

a splitted main diffraction peak at $d = 2.713$ Å and $d = 2.681$ Å ((1 1 0) and (1 0 4) planes). The two structures only differ by the distortion of the iron coordination octahedral alignment compared to cobalt.

The crystalline structure of the mixed Co–Fe perovskites was determined by XRD. The diffractograms of the $LaCo_xFe_{(1-x)}O_3$ series calcined at 1100 °C are presented in Fig. 3.

For intermediate perovskites the main reflection is single for $x = 0.25$ and 0.4, and splitted for higher values of x. The crystalline phase is single, no other oxide was detected.

The lattice parameters were refined in the orthorhombic system (for $x = 0.25$, 0.4) or in the rhombohedral system (for $x = 0.5$, 0.6 and 0.75). $LaCo_{0.50}Fe_{0.50}O_3$ was refined in the rhombohedral system which is its majoritary crystalline phase. The normalized cell volumes versus x are reported in Table 2.

The preparation method by the propionate synthesis leads, after calcination at relatively low calcination temperatures, to two solid solutions: one isomorphic to $LaFeO_3$ for $x < 0.5$ and one isomorphic to $LaCoO_3$ for $x \geq 0.5$.

This result is in accordance with that obtained by Traversa et al. [19] who studied La–Co–Fe perovskites prepared by the thermal decomposition of the cyanide-bridged heteronuclear complexes $La[Fe_xCo_{1-x}(CN_6)] \cdot nH_2O$.

Table 2
Cell parameters of $LaCo_xFe_{(1-x)}O_3$ perovskites

Perovskites	Crystallographic system	a parameter (Å)	b parameter (Å)	c parameter (Å)	Normalized cell volume (Å^3)
$LaCoO_3$	R	5.44	5.44	13.10	56.05
$LaCo_{0.75}Fe_{0.25}O_3$	R	5.45	5.45	13.11	56.25
$LaCo_{0.60}Fe_{0.40}O_3$	R	5.47	5.47	13.27	57.43
$LaCo_{0.50}Fe_{0.50}O_3$	R + O (traces)	5.51	5.51	13.29	58.18
$LaCo_{0.40}Fe_{0.60}O_3$	O	5.51	7.81	5.51	59.30
$LaCo_{0.25}Fe_{0.75}O_3$	O	5.55	7.83	5.53	59.96
$LaFeO_3$	O	5.56	7.86	5.56	60.78

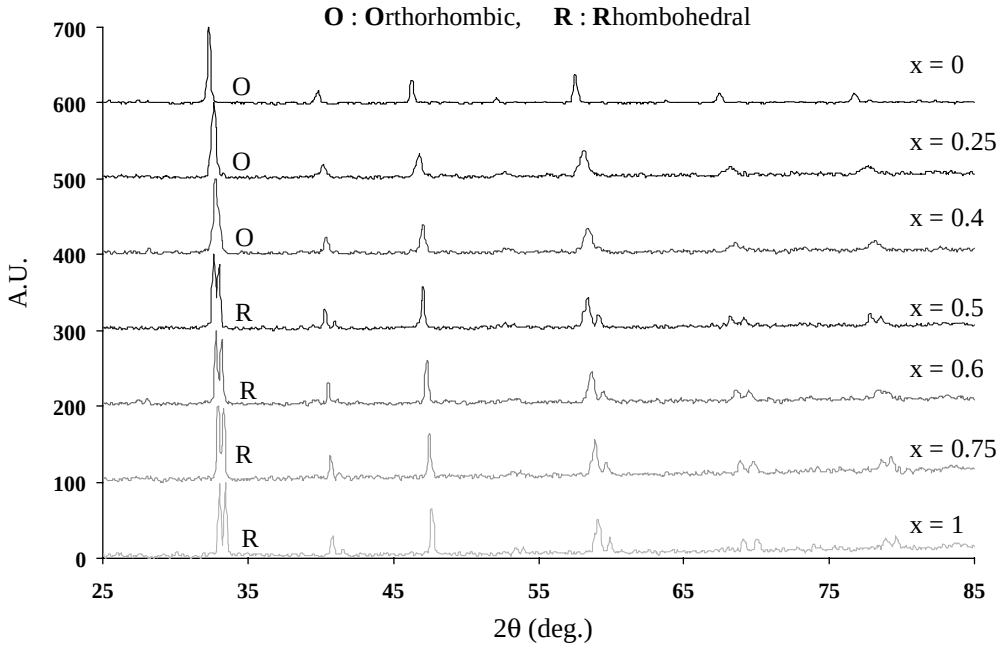

Fig. 3. XRD spectra of $LaCo_xFe_{(1-x)}O_3$ after calcination at 1100 °C.

3.4. TPR

The metal phase being the active phase in the Fischer–Tropsch synthesis, attention was paid to the reducibility of the mixed perovskites.

Their reduction was first followed by TPR. The hydrogen consumption profiles are presented in Fig. 4 for the series of perovskites calcined at 750 °C.

The reduction of $LaFeO_3$ begins at 750 °C and is not complete at 900 °C. For all other perovskites, the reduction proceeds in two steps. The first reduction area is observed at low temperatures between 300 and 500 °C. The second only begins around 570 °C and ends the earlier, the higher cobalt content the perovskite presents. These two reduction steps are well separated in temperature: at least 70 °C. As consequence, all the partially reduced cobalt-containing perovskites are stable under reducing conditions between 500 and 570 °C. This stability of partially reduced oxides would allow their use as stable catalyst for Fischer–Tropsch synthesis.

The volume of hydrogen consumed during the first reduction area is given in Fig. 5 as a function of the cobalt content x. The linear increase of hydrogen consumption with x indicates that only cobalt would be affected during the partial reduction of the mixed perovskites. Iron ions would only be reduced in the second reduction area at higher temperature.

3.5. Magnetic measurements and formulae of the reduced catalysts

To make sure that metal cobalt particles arise from this reduction, magnetic measurements under a H_2 flow have been carried out. The evolution of the magnetization during the reduction of the catalysts under the same conditions as in TPR experiments (H_2 flow, temperature) is presented in Fig. 6 for $LaCo_{0.4}Fe_{0.6}O_3$ and $LaCo_{0.75}Fe_{0.25}O_3$.

For $x = 0.4$ as well as for all other orthorhombic perovskites, the magnetization curve shows two jumps at 410 and 625 °C due to the formation of a ferromagnetic phase. The first increase at 410 °C corresponds to the first reduction area observed in TPR. The ferromagnetic phase formed after the partial reduction of orthorhombic perovskites is then attributed to metallic cobalt (ferromagnetic, 161 emu g^{-1} at room temperature) [20].

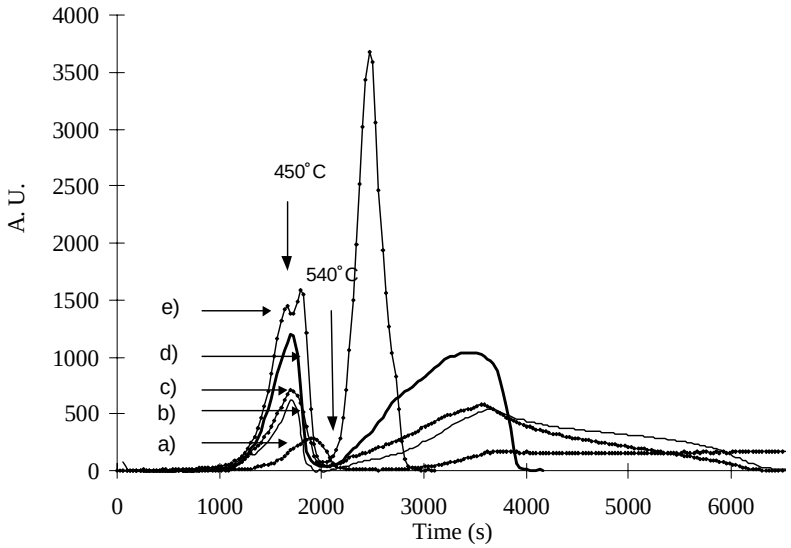

Fig. 4. TPR profiles of perovskites calcined at 750 °C: (a) $LaFeO_3$, (b) $LaCo_{0.25}Fe_{0.75}O_3$, (c) $LaCo_{0.50}Fe_{0.50}O_3$, (d) $LaCo_{0.75}Fe_{0.25}O_3$, (e) $LaCoO_3$.

For $x = 0.75$ and for all other rhombohedral perovskites, although the hydrogen consumption in the first area of reduction is higher, no magnetization increase is observed around 400 °C. The metal phase is only formed in the second area of reduction, after 600 °C.

Although more cobalt-containing, rhombohedral perovskites do not lead to metal cobalt particles after their partial reduction, excluding any application in Fischer–Tropsch synthesis. At 400 °C, the hydrogen consumption is then only due to the reduction of Co^{III} into Co^{II} in the perovskite phase.

Active Fischer–Tropsch catalysts arise from the partial reduction of $LaCo_xFe_{1-x}O_3$ orthorhombic perovskites ($x < 0.5$). To characterize these catalysts under their partially reduced form, the reduction procedure has been optimized and validated by TPR on the reduced samples.

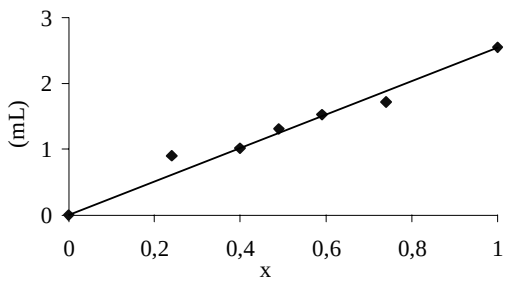

Fig. 5. Volume of hydrogen (V_1) consumed during the first area of reduction for perovskites calcined at 750 °C.

The oxides were reduced by heating at 450 °C (2 °C min^{-1}) for 90 min under a 10% H_2/He flow. After the reduction, a TPR was carried out and compared to that of the unreduced oxides. The two TPR profiles are given in Fig. 7 for $LaCo_{0.40}Fe_{0.60}O_3$.

It clearly appears that the first reduction zone has completely disappeared for the partially reduced oxide, whereas the second zone has not been affected by the reduction process. The reducing treatment established for this perovskite series is then efficient to reproduce the first reduction step.

The partially reduced oxides were first characterized by XRD. Although Co^0 was evidenced by magnetic studies, no metal was observed. More, the perovskite structure is fully preserved despite cobalt deficiency.

In order to quantify the amount of Co^0 in the partially reduced orthorhombic perovskites, magnetization cycles have been performed on samples after reducing treatment. Assuming that only metal cobalt is formed, the magnetization value accounts for the amount of Co^0 in the reduced sample.

The cycles are presented in Fig. 8 (curves a and b) for $x = 0.25$ and 0.40 (calcination at

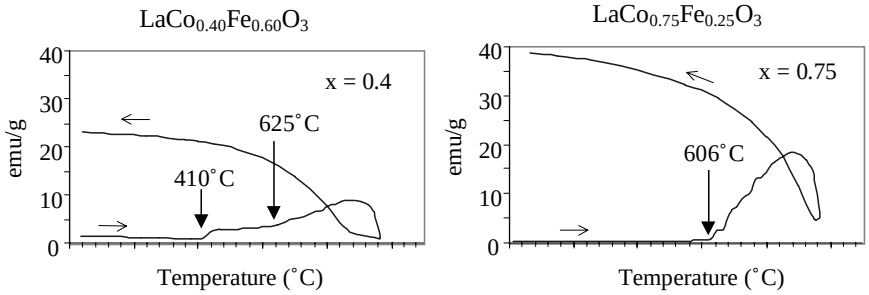

Fig. 6. Evolution of the magnetization versus temperature under reducing flow.

750 °C), respectively. The saturation magnetization is 4.20 emu g^{-1} for $LaCo_{0.25}Fe_{0.75}O_3$ and 3.30 emu g^{-1} for $LaCo_{0.40}Fe_{0.60}O_3$ calcined at 750 °C. These values correspond, respectively, to 2.61 and 2.05 wt.% of Co^0.

To enhance the amount of metal phase extractable from the orthorhombic perovskites, the same experiments (TPR, control of the partial reduction, magnetization cycles after partial reduction) have been carried out on for $LaCo_{0.25}Fe_{0.75}O_3$ and for $LaCo_{0.40}Fe_{0.60}O_3$ calcined at 600 °C. The magnetization cycles are given in Fig. 8 (curves c and d). The magnetization is clearly increased by the lowering of the calcination temperature, from 4.20 to 11.65 emu g^{-1} for $LaCo_{0.25}Fe_{0.75}O_3$, and from 3.30 to 13.85 emu g^{-1} for $LaCo_{0.40}Fe_{0.60}O_3$. The embrittlement of the crystalline structure allows a deeper reduction of the oxides.

Taking into account the volume of hydrogen consumed in the first area of reduction and the magnetization value after partial reduction, formulae of the reduced perovskites have been established assuming that iron is not affected by the reduction at 450 °C. The formulae are presented in Table 3.

We have to point out that for $LaCo_{0.25}Fe_{0.75}O_3$ at 600 °C the former assumption was clearly not convenient. The magnetization is too high to be only due to complete reduction of cobalt into Co^0 and corresponds to an alloy $(Co_{0.85}Fe_{0.15})^0$. This also explains very well why the same perovskite at 750 °C

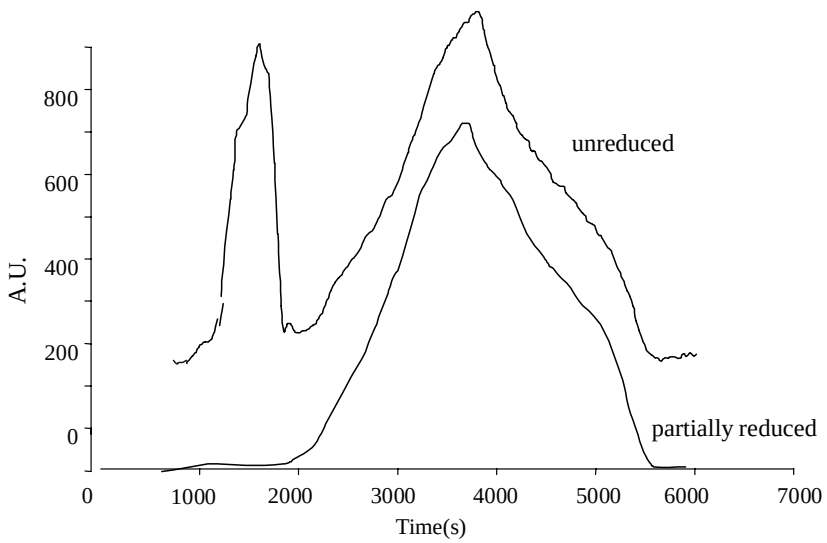

Fig. 7. TPR profile of $LaCo_{0.4}Fe_{0.6}O_3$ calcined at 750 °C before and after partial reduction.

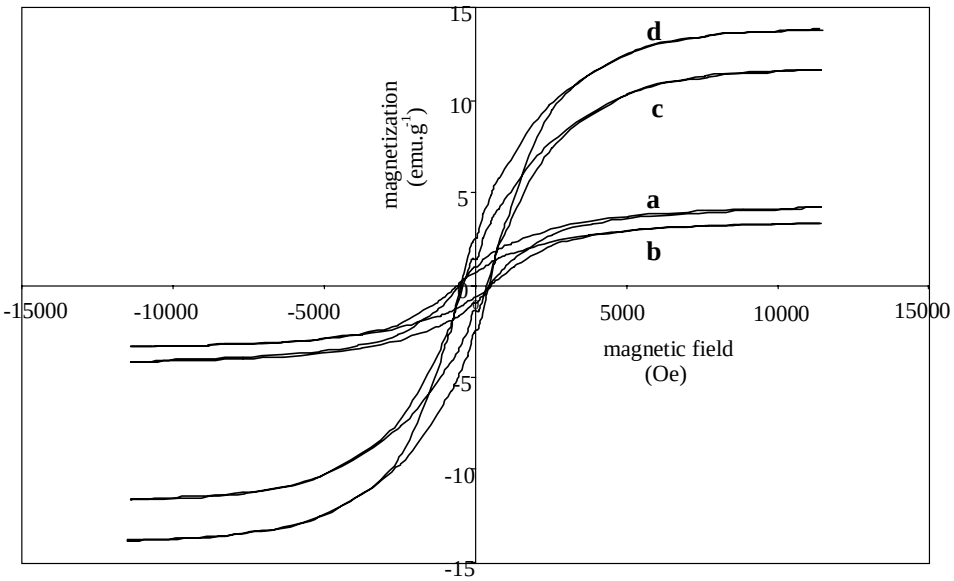

Fig. 8. Magnetization cycles of partially reduced samples: (a) $x = 0.25$ calcined at 750 °C, (b) $x = 0.40$ calcined at 750 °C, (c) $x = 0.25$ calcined at 600 °C, (d) $x = 0.40$ calcined at 600 °C.

consumed more H_2 than expected if only cobalt is reduced in the first zone of TPR (see Fig. 5) and why its magnetization value after partial reduction is higher than that of $LaCo_{0.40}Fe_{0.60}O_3$ at 750 °C although richer in cobalt: the metal extracted by partial reduction of this perovskite would contain part of iron metal (15%) which enhances the magnetization of the sample (Fe^0 is ferromagnetic, 220 emu g^{-1} [21]).

For rhombohedral mixed perovskites, the partial reduction completely reduced Co^{3+} into Co^{2+} in the B site of the structure. Iron is not affected at all by the treatment. As soon as the iron amount is higher than 50% in the B sites (orthorhombic), the perovskite is

Table 3
Detailed formulae of the partially reduced perovskites

Perovskite	T[a] (°C)	V_1[b] (ml)	Ms[c] (emu g^{-1})	V_{metal}[d] (ml)	Formula of the partially reduced perovskite (1 h, 450 °C)
$LaFeO_3$	750	0	0	0	$LaFeO_3$
$LaCo_{0.24}Fe_{0.76}O_3$ ($x = 0.25$)	750	0.90	4.20	0.76	$0.11Co^0/LaCo_{0.06}{}^{2+}Co_{0.07}{}^{3+}Fe_{0.76}{}^{3+}O_{2.80}$ or $0.11(Co_{0.85}{}^0Fe_{0.15}{}^0)/LaCo_{0.07}{}^{2+}Co_{0.08}{}^{3+}Fe_{0.76}{}^{3+}O_{2.80}$
	600	2.53	11.65	1.97	$0.28(Co_{0.85}{}^0Fe_{0.15}{}^0)/LaFe_{0.19}{}^{2+}Fe_{0.53}{}^{3+}O_{2.49}$
$LaCo_{0.4}Fe_{0.6}O_3$ ($x = 0.40$)	750	1.02	3.30	0.58	$Co_{0.08}{}^0/LaCo_{0.19}{}^{2+}Co_{0.13}{}^{3+}Fe_{0.60}{}^{3+}O_{2.78}$
	600	2.45	13.85	2.45	$Co_{0.35}{}^0/LaCo_{0.05}{}^{3+}Fe_{0.60}{}^{3+}O_{2.40}$
$LaCo_{0.49}Fe_{0.51}O_3$	750	1.31	0	0	$LaCo_{0.49}{}^{2+}Fe_{0.51}{}^{3+}O_{2.63}$
$LaCo_{0.59}Fe_{0.41}O_3$	750	1.53	0	0	$LaCo_{0.59}{}^{2+}Fe_{0.41}{}^{3+}O_{2.63}$
$LaCo_{0.74}Fe_{0.26}O_3$	750	1.72	0	0	$LaCo_{0.74}{}^{2+}Fe_{0.26}{}^{3+}O_{2.63}$
$LaCoO_3$	750	2.55	5	0.34	$Co_{0.05}{}^0/LaCo_{0.95}{}^{2+}O_{2.45}$

[a] The calcination temperature.
[b] The volume of hydrogen consumed in the first area of TPR for 50 mg of sample.
[c] The highest magnetization.
[d] The volume of hydrogen calculated for 50 mg of sample to form the amount of metal determined from magnetization cycles.

strong enough to allow the expulsion of B cations via Co^0 particle formation under hydrogen.

The maximal amount of metal available from the perovskites we studied is obtained for $x = 0.4$ at 600 °C and is of 8.6 wt.% of Co^0. In this catalyst, cobalt is almost totally extracted of the initial oxide, without any breakdown of the perovskite structure.

3.6. CO disproportionation

To foresee the Fischer–Tropsch activity of the partially reduced perovskites, their ability to dissociate carbon monoxide has been studied according to the following scheme:

$$CO \rightarrow C_s + O_s \quad \text{and} \quad CO + O_s \rightarrow CO_2$$

CO is admitted by pulses at 350 °C on the reduced catalysts.

CO conversion is presented in Fig. 9 for the series calcined at 750 °C. The less efficient catalysts for CO dissociation are the rhombohedral perovskites. Within this series CO conversion increases with the cobalt content of the perovskite from 2% for $x = 0.50$ to almost 5% for $x = 0.75$. $LaCoO_3$ and orthorhombic perovskites present better activities: 7.3% of CO conversion for reduced $LaCoO_3$ (contains 1.1 wt.% of Co^0), 10% for reduced $LaCo_{0.25}Fe_{0.75}O_3$ (contains either 2.6% of Co^0 or 2.6% of the alloy $(Co_{0.85}Fe_{0.15})^0$), with a maximal conversion of 12% for reduced $LaCo_{0.40}Fe_{0.60}O_3$ (contains 2.1 wt.% of Co^0).

When comparing the two last systems it appears that despite its higher metal content, the activity of the catalyst $x = 0.25$ is lower. This tends to confirm the hypothesis of an alloy $(Co_{0.85}Fe_{0.15})^0$ by partial reduction even when calcined at 750 °C. The presence of iron in the metal phase would dilute the Co^0 more active phase for CO conversion [22–24].

The comparison of activity for $x = 0.40$, the most active catalyst of the series at 750 °C, with the same system calcined at lower temperature of 600 °C is given in Fig. 10. With increasing Co^0 content CO conversion increases from 12% for the perovskite calcined at 750 °C (2.1 wt.% Co^0) to 28% for the perovskite calcined at 600 °C (8.6 wt.% of Co^0). The beneficial effect of lower calcination treatment on the amount

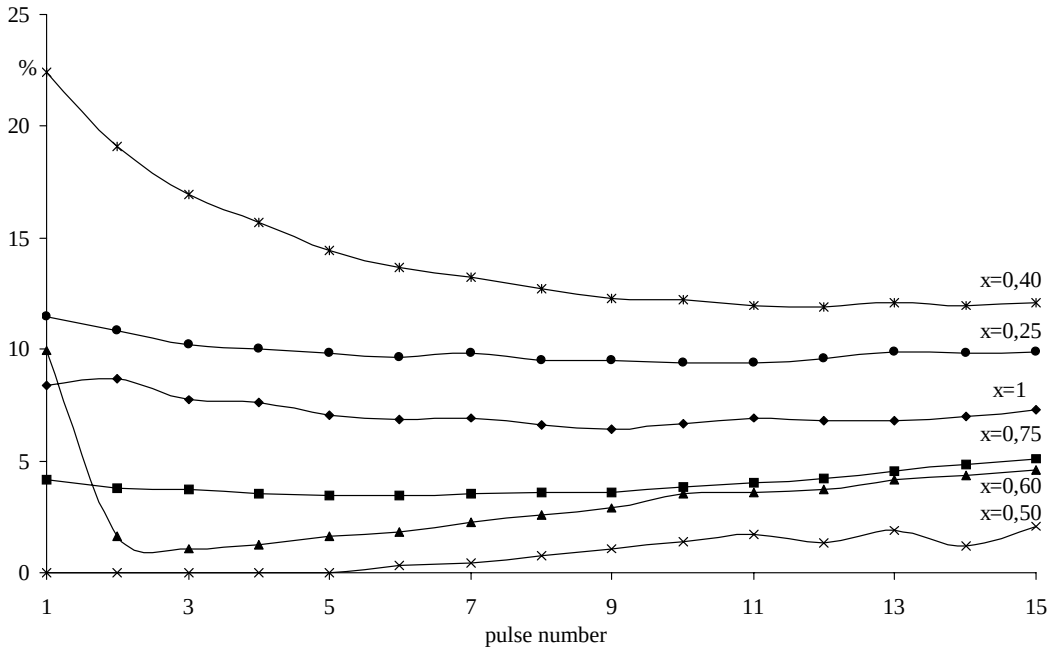

Fig. 9. CO conversion as a function of pulse number for the perovskites calcined at 750 °C.

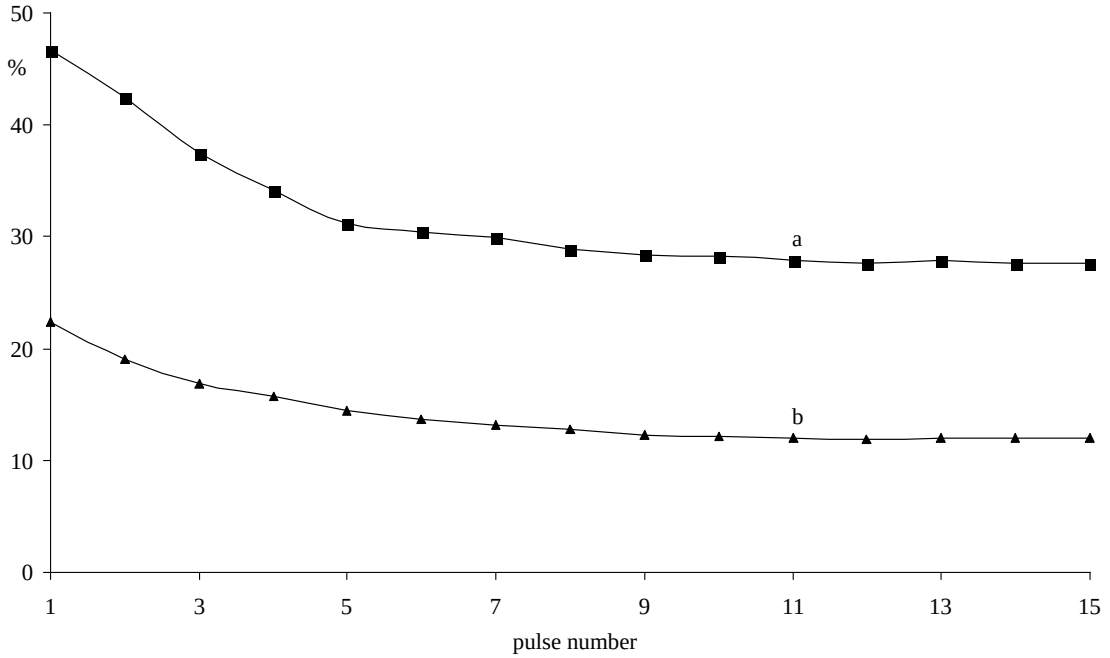

Fig. 10. CO conversion as a function of the pulse number for the perovskite: (a) $x = 0.40$ calcined at 600 °C, (b) $x = 0.40$ calcined at 750 °C.

of metal extractable of the oxide clearly improves the potential activity of the catalysts.

3.7. Fischer–Tropsch synthesis

The improvement of activity in CO dissociation due to higher metal cobalt has been verified in the Fischer–Tropsch synthesis. Conversion of CO and product distribution are presented in Table 4 for the perovskites $x = 0.40$ calcined at 600 and 750 °C.

At isoconversion of almost 3.5% the reaction temperature is lower for the perovskite $x = 0.40$ calcined at 600 °C than for that calcined at 750 °C (250 compared to 280 °C). At 260 °C, the catalysts at 750 °C is inactive whereas the CO conversion observed with the same catalyst calcined at 600 °C is more than 6%.

Table 4
Catalytic results in Fischer–Tropsch reaction at various temperatures of $LaCo_{0.40}Fe_{0.60}O_3$ ($x = 0.40$) calcined at 600 and 750 °C

	Catalyst				
	$Co_{0.35}{}^{0}/LaCo_{0.05}{}^{3+}Fe_{0.60}{}^{3+}O_{2.40}$ (8.6%) (600 °C)			$Co_{0.08}{}^{0}/LaCo_{0.19}{}^{2+}Co_{0.13}{}^{3+}Fe_{0.60}{}^{3+}O_{2.78}$ (2.0%) (750 °C)	
	240 °C	250 °C	260 °C	270 °C	280 °C
CO conversion (%)	2.4	3.5	6.1	1.9	3.7
Molar selectivity in hydrocarbons (%)	70.2	70.9	68.4	69.8	68.8
Molar selectivity in CO_2 (%)	12.5	17.9	23.7	20.0	24.8
Molar selectivity in oxygenated products (%)	17.3	11.2	7.9	10.2	6.4
Weight distribution in the HC fraction					
CH_4 (%)	32.8	39.3	44.5	44.4	52.3
C_2–C_4 (%)	41.2	44.8	42.4	41.1	36.2
$C_5{}^{+}$ (%)	26	15.9	13.1	14.5	11.5
Olefins (%) in the C_2–C_4 fraction	76.7	73.0	67.7	71.4	63.0

As expected after CO dissociation studies, higher Co^0 content in the catalyst strongly enhances the activity in the Fischer–Tropsch reaction.

The molar selectivity into hydrocarbons is almost the same for the two catalysts at various temperatures and takes values around 70%, it does not depend on the metal content in the catalyst and is not sensitive to reaction temperature (within the range we studied here). Reaction temperature strongly influences the CO_2 formation. For example, the molar selectivity into CO_2 increases from 12.5% at 240 °C to 23.7% at 260 °C for the perovskite calcined at 600 °C. This phenomenon is counterbalanced by a lower oxygenated product formation at higher reaction temperature: from 17.3 to 7.9% of the molar selectivity in the same conditions.

Only few data are available in literature concerning the formation of oxygenated products [25] as by-products in the Fischer–Tropsch synthesis towards hydrocarbons. They are generally not mentioned in the catalytic results. In our case the oxygenated products are methanol, ethanol and acetaldehyde. Ethanol is always the majoritary product and represents almost 70% in this fraction. The formation of such products could be accounted for by the participation of the deficient perovskite oxide support to the catalytic reaction.

Within the hydrocarbon products, the major fraction is always the light C_2–C_4 hydrocarbons for the catalyst calcined at 600 °C. For this system, the weight percentage of C_2–C_4 varies between 41 and 45%. For the other catalyst, the amount of C_2–C_4 is lower (between 36 and 41%) because of the higher reaction temperature which favors methane formation. Although increasing reaction temperatures also decreases the olefin ratio in this fraction, the Fischer–Tropsch selectivity is always largely directed towards light olefins. For the most active catalyst, olefins represent 76.7% of the C_2–C_4 fraction for the test at 240 °C and 67.7% at 260 °C. The good selectivity towards light olefins is not usual for Co^0-based systems, but is more characteristic of Fe^0 or $(CoFe)^0$-based catalysts [26–29]. The same conclusion can be drawn about the values of CO_2 selectivities obtained with our systems which are rather high for Co^0-based catalysts [23,30,31]. These behaviors and the non-negligible formation of oxygenated products are consistent with a role played by the iron-containing perovskite in the Fischer–Tropsch reaction.

The increasing metal content from 2 to 8.6% does not affect the product distribution which accounts in the two catalysts for small Co^0 particle size. This could explain why the metal phase could not be detected by XRD despite its quite high content.

The cobalt particle size can be estimated from magnetic results. The cycles of the reduced perovskites $x = 0.40$ calcined at 600 and 750 °C are presented in Fig. 8(b) and (d), respectively. A small coercitive field, characteristic of ferromagnetic phase, of almost 600 Oe exists on the magnetization curves. But the saturation of the magnetization is difficult to reach, which is characteristic of a superparamagnetic behavior [32–34]. For cobalt metal particles, superparamagnetism is encountered for particle size less than 6 nm [20]. All the metal cobalt particles arise from the reduction of the same initial structure, we can then admit that their mean size is at the limit of the two magnetic behaviors: around 10 nm. Even if the amount of Co^0 is high (8.6%), the nanometer size of the particles is preserved, ensuring a good selectivity towards light olefins in the Fischer–Tropsch reaction.

4. Conclusions

The preparation method based on propionate polymerization in solution allows the crystallization of mixed $LaCo_xFe_{1-x}O_3$ perovskites at 600 °C.

The crystalline structure of the oxides can be controlled by modifying the Co/Fe ratio in the preparation. For $x \geq 0.5$ the perovskites are rhombohedral, isomorphic of $LaCoO_3$. For $x < 0.5$, the perovskites are orthorhombic, isomorphic of $LaFeO_3$.

The reducibility of the mixed Co–Fe lanthanum perovskites depends on their crystalline structure.

For mixed orthorhombic perovskites, the partial reduction at 420 °C leads to a metal phase well dispersed on a stable cation-deficient perovskite. For mixed rhombohedral perovskites, the same reducing treatment does not lead to metal particles but only reduces Co^{3+} of the perovskite into Co^{2+}.

In order to enhance the amount of extractable Co^0 from the orthorhombic perovskites, the influence of the calcination temperature of the oxide was studied. The amount of metal is directly related to the stability of the precursor oxide. For $LaCo_{0.40}Fe_{0.60}O_3$, the partial reduction of the perovskite calcined at 750 °C generates a 2 wt.% Co^0 catalyst, whereas for the perovskite calcined at 600 °C, 8.6 wt.% of Co^0

were extracted. The remaining oxide is nearly free of cobalt, and stable despite the high cation deficiency: $LaFe_{0.60}O_{2.40}$. This enhancement of the metal phase does not affect the Co^0 particle size which remains lower than 10 nm.

This small particle size is ensured by the controlled reduction of a well crystalline definite structure. The CO conversion is strongly dependent on the metal content of the catalyst. Higher metal content allows the decrease of the reaction temperature, which is more favorable to lower CO_2 selectivities and higher olefin contents in the C_2–C_4 hydrocarbon fraction.

The F–T results (rather high CO_2 selectivities compared to other Co^0-based catalysts, non-negligible formation of ethanol) tend to show that the iron-containing deficient perovskite plays a role in the FT reaction. Overall, this work shows the high potential of (Co–Fe) perovskites for C_2–C_4 olefins formation.

References

[1] H. Arai, T. Yamada, K. Eguchi, T. Seiyama, Appl. Catal. 26 (1986) 265.
[2] T. Nitadori, M. Misono, J. Catal. 93 (1985) 93.
[3] K.S. Chan, J. Ma, S. Jaenicke, G.K. Chuah, Appl. Catal. A 107 (1994) 337.
[4] R. Doshi, C.B. Alcock, J.J. Carberry, Catal. Lett. 18 (1993) 337.
[5] M. Teymouri, C. Petit, J.L. Rehspringer, S. Libs, E. Bagherzhadeh, A. Kiennemann, J. Mater. Sci. 30 (1995) 3005.
[6] C. Petit, A. Kiennemann, P. Chaumette, O. Clause, French Patent 92/11638 (28 September 1992).
[7] H. Provendier, C. Petit, A.C. Roger, A. Kiennemann, Stud. Surf. Sci. Catal. 118 (1998) 285.
[8] G. Rodriguez, A.C. Roger, L. Udron, L. Bedel, L. Carballo, A. Kiennemann, A.C.S. Fuel, Div. Preprints 47 (1) (2002) 260.
[9] J.O. Pentuchi, M.A. Ulla, J.A. Marcos, E.A. Lombardo, J. Catal. 70 (1981) 536.
[10] K. Ichimura, Y. Inoue, I. Yasumori, Bull. Chem. Soc. Jpn. 54 (1981) 1787.
[11] Powder Diffraction File, International Center for Diffraction Data, File 25-1060.
[12] Powder Diffraction File, International Center for Diffraction Data, File 37-1493.
[13] A.R. Chakhmouradian, R.M. Mitchell, P.C. Burns, J. Alloys Comp. 307 (2000) 149.
[14] D. Waller, J.A. Lane, J.A. Kilner, B.C.H. Steele, Mater. Lett. 27 (1996) 225.
[15] D. Waller, J.A. Lane, J.A. Kilner, B.C.H. Steele, Solid State Ionics 86–88 (1996) 767.
[16] G.C. Kostogloudis, C. Ftikos, Solid State Ionics 126 (1999) 143.
[17] J.L. Rehspringer, J.C. Bernier, Mater. Res. Soc. Symp. Proc. 72 (1986) 67.
[18] H. Provendier, C. Petit, J.-L. Schmitt, A. Kiennemann, J. Mater. Sci. 34 (1999) 4121.
[19] E. Traversa, P. Nunziante, M. Sakamoto, Y. Sadaoka, R. Montanari, Mater. Res. Bull. 33 (5) (1998) 673.
[20] X.M. Lin, C.M. Sorensen, K.J. Klabunde, G.C. Hadjipanayis, Langmuir 14 (1998) 7140.
[21] CRC Handbook of Chemistry and Physics, 47th ed., 1966, E-101.
[22] D.J. Duvenhage, N.J. Coville, Appl. Catal. A 153 (1997) 43.
[23] M.E. Dry, Catal. Today 71 (2002) 227.
[24] K. Tabata, I. Matsumoto, S. Kohiki, J. Mater. Sci. 22 (1987) 1882.
[25] H. Araï, K. Mitsuichi, T. Seiyama, Chem. Lett. (1984) 1291.
[26] P. Villeger, J. Barrault, J. Barbier, G. Leclercq, R. Maurel, Bull. Soc. Chim. Fr. 9–10 (1979) 414.
[27] T. Ishihara, K. Eguchi, H. Arai, Appl. Catal. 30 (1987) 225.
[28] A.A. Chen, M. Kaminsky, G.L. Geoffroy, M.A. Vannice, J. Phys. Chem. 90 (1986) 4810.
[29] F. Tihay, G. Pourroy, M. Richard-Plouet, A.C. Roger, A. Kienneman, Appl. Catal. A 206 (1) (2001) 29.
[30] J.A. Amelse, L.H. Schwartz, J.B. Butt, J. Catal. 72 (1981) 95.
[31] B. Ernst, L. Hilaire, A. Kiennemann, Catal. Today 50 (1999) 413.
[32] B. Imelik, J.C. Védrine, Les techniques physiques d'étude des catalyseurs, Technip Ed., 1998, p. 791.
[33] A. Herpin, Théorie du magnétisme, PUF Ed., 1968.
[34] D.H. Martin, Magnetism in Solids, MIT Press, Cambridge, MA, 1967.